



# Earth's Future

## RESEARCH ARTICLE

10.1029/2018EF000937

### Key Points:

- Without mitigation of CO<sub>2</sub> emissions, the forecast increase (2015–2100) of global soil respiration rates will increase to 0.11 Pg C year<sup>-1</sup>
- If temperature rises by 3 °C by 2100, R<sub>s</sub> sensitivity in warm regions will decrease substantially while sensitivity in colder regions will increase
- A single model underestimated R<sub>s</sub> in cold regions but overestimated R<sub>s</sub> in arid and temperate regions when compared with the climate-specific model

### Supporting Information:

- Supporting Information S1

### Correspondence to:

J. Jian,  
jinshi@vt.edu

### Citation:

Jian, J., Steele, M. K., Day, S. D., & Thomas, R. Q. (2018). Future global soil respiration rates will swell despite regional decreases in temperature sensitivity caused by rising temperature. *Earth's Future*, 6. <https://doi.org/10.1029/2018EF000937>

Received 21 MAY 2018

Accepted 5 OCT 2018

Accepted article online 12 OCT 2018

## Future Global Soil Respiration Rates Will Swell Despite Regional Decreases in Temperature Sensitivity Caused by Rising Temperature

Jinshi Jian<sup>1</sup> , Meresith K. Steele<sup>1</sup> , Susan D. Day<sup>2,3</sup> , and R. Quinn Thomas<sup>2</sup>

<sup>1</sup>School of Plant and Environmental Sciences, Virginia Tech, Blacksburg, VA, USA, <sup>2</sup>Department of Forest Resources and Environmental Conservation, Virginia Tech, Blacksburg, VA, USA, <sup>3</sup>Department of Horticulture, Virginia Tech, Blacksburg, VA, USA

**Abstract** Between 1960 and 2014, the global soil respiration (R<sub>SG</sub>) flux increased at a rate of 0.05 Pg C year<sup>-1</sup>; however, future increase is uncertain due to variations in projected temperature and regional heterogeneity. Regional differences in the sensitivity of soil respiration (R<sub>s</sub>) to temperature may alter the overall increase in rates of R<sub>s</sub> because the R<sub>s</sub> rates of some regions may decelerate while others continue to rise. Using monthly global R<sub>s</sub> data, we modeled the relationship between R<sub>s</sub> and temperature for the globe and eight climate regions and estimated R<sub>SG</sub> between 1961 and 2100 using historical (1961–2014) and future (2015–2100) temperature data [Representative Concentration Pathways (RCP2.6 and RCP8.5)]. Importantly, our approach allowed for estimation of regional sensitivity, where respiration rates may peak or decline as temperature rises. Estimated historical R<sub>SG</sub> increase (0.05 Pg C year<sup>-1</sup>) was similar to the R<sub>SG</sub> increase of previous estimates. However, under the RCP8.5 scenario, which estimates approximately 3 °C of warming globally, the forecasted acceleration of R<sub>SG</sub> increased to an average of 0.12 Pg C year<sup>-1</sup>. Under RCP8.5, the temperature sensitivity of R<sub>s</sub> declined in the arid, winter-dry temperate, and tropic. These regional declines were offset by increased R<sub>s</sub> sensitivity and fluxes from the boreal and polar regions. In contrast, under RCP2.6 R<sub>SG</sub> decelerated slightly from current rates. If rising greenhouse gas emission remains unmitigated, future increases in R<sub>SG</sub> will be much faster than current and historical rates, thereby possibly enhancing future losses of soil carbon and contributing to positive feedback loops of climate change.

**Plain Language Summary** Between 1960 and 2014, the global CO<sub>2</sub> flux increased at a rate of 0.05 Pg carbon per year; however, future increase of CO<sub>2</sub> emission from soil is uncertain. Regional differences in the sensitivity of soil CO<sub>2</sub> efflux to temperature change may alter the overall soil CO<sub>2</sub> emission. We modeled the relationship between soil CO<sub>2</sub> efflux and temperature for the globe and eight climate regions, and estimated global soil CO<sub>2</sub> efflux between 1961 and 2100 using historical temperature data (1961–2014) and future temperature (2015–2100, RCP 2.6 and 8.5). Estimated historical global soil CO<sub>2</sub> efflux acceleration (0.05 Pg carbon per year) was similar to the global soil CO<sub>2</sub> efflux acceleration of previous estimates. However, under the RCP8.5, which estimates approximately 3°C of warming globally, the forecasted acceleration of global soil CO<sub>2</sub> efflux increased to 0.12 Pg carbon per year. In contrast, under the RCP 2.6 scenario, the global soil CO<sub>2</sub> efflux rate decelerated slightly from current rates. If rising greenhouse gas emission remains unmitigated, future acceleration of global soil CO<sub>2</sub> efflux will be much faster than current and historical rates, thereby enhancing future losses of soil carbon and contributing to accelerate climate change.

## 1. Introduction

Soil respiration (R<sub>s</sub>), the production of carbon dioxide from the soil when plant roots, microbes, and fauna respire, is the second largest carbon flux between the land and atmosphere (Raich & Schlesinger, 1992; Zhao et al., 2017). From 1961 to 2011, global fluxes of R<sub>s</sub> (R<sub>SG</sub>) increased by 0.04 to 0.10 Pg C year<sup>-1</sup> (Bond-Lamberty & Thomson, 2010a, 2010b; Hashimoto et al., 2015; Zhao et al., 2017). While these historical trends provide some insight into the future rate of change in R<sub>s</sub>, the trajectory of R<sub>SG</sub> remains uncertain, as global temperature increases. This uncertainty in R<sub>SG</sub> is due, in part, to a lack of knowledge regarding how regional R<sub>s</sub> rates will respond to rising temperature. Globally, average temperature over land has increased by 0.1 °C per decade since 1950 (Hartmann et al., 2013). Regionally, however, temperature changes may

©2018. The Authors.

This is an open access article under the terms of the Creative Commons Attribution-NonCommercial-NoDerivs License, which permits use and distribution in any medium, provided the original work is properly cited, the use is non-commercial and no modifications or adaptations are made.

differ significantly from global averages. For example, temperature has risen much faster than the global average in high-latitude regions, 0.6 °C per decade over the last 30 years (Hartmann et al., 2013). Since temperature is a critical driver of  $R_S$ , assumptions regarding the sensitivity of  $R_S$  to temperature change significantly affect predictions of  $R_{SG}$  rates, and how those rates will respond to global warming (Davidson & Janssens, 2006; Janssens et al., 2001; Trumbore, 2006). While  $R_S$  generally increases with temperature,  $R_S$  rate can level off or begin to decline when temperature rises above a certain threshold (Lellei-Kovacs et al., 2011; Parker et al., 1983). That threshold temperature differs with climates and biomes as a result of varying precipitation, soil moisture, primary production, and soil carbon (Hursh et al., 2017). At the regional scale, a recent study found that  $R_S$  rates in specific biomes are already less sensitive to temperature increases than during past decades (Zhao et al., 2017). Higher temperature in the future may further dampen the temperature sensitivity of  $R_S$  in large regions. As a result, the declining  $R_S$  in warm climates may help to dampen  $R_{SG}$  as temperature increases. However, higher temperature may also increase  $R_S$  in colder regions and overwhelm other regional declines. Currently, we lack models that incorporate the variation in temperature sensitivity, which impairs accurate assessment of how heterogeneity in regional-scale sensitivity of  $R_S$  may influence future  $R_{SG}$  fluxes and feedbacks to climate change.

The temperature sensitivity of  $R_S$  can be quantified by a  $Q_{10}$  function, where  $Q_{10}$  is a measure of the change in rate of  $R_S$  as temperature increases 10 °C (Lloyd & Taylor, 1994). In ecosystem models, constant  $Q_{10}$  functions (a rule of thumb is  $Q_{10} = 2$ ) have been widely used (Conant et al., 2011). Likewise, empirical models that estimate  $R_S$  at the global scale also assume either a linear relationship or constant  $Q_{10}$  relationships between  $R_S$  and temperature (Raich & Potter, 1995; Raich et al., 2002). Under constant  $Q_{10}$  models,  $R_{SG}$  estimates increased with increasing temperature across the entire globe (Bond-Lamberty & Thomson, 2010a, 2010b). However, numerous laboratory and warming experiments demonstrate that  $R_S$  rates decline when temperature rises above specific optima (Bradford et al., 2008; Crowther & Bradford, 2013; Frey et al., 2013; Luo et al., 2001; Sistla et al., 2013). For example, a meta-analysis of  $R_S$  measurements from 27 experimental field-warming studies found the quadratic model best explained how  $R_S$  responds to temperature in both control and warming sites. Moreover, they detected a threshold of approximately 25.0 °C after which  $R_S$  began to slow (Carey et al., 2016). Furthermore, another meta-analysis using soils originating from different ecosystems (including forest, grassland, cultivated, tundra, peat land, and polar), incubated from a few hours to 720 days and from −15 to 55 °C, found that  $Q_{10}$  values of  $R_S$  ranged from 0.5 to 300, and the  $Q_{10}$  values negatively correlated to soil temperature when temperature was below 25 °C (Hamdi et al., 2013). These studies suggest that higher regional temperature should result in a leveling off or decline in  $R_S$  rate when temperature is over the optimum, which is more likely to occur in the future as temperature rises.

Fluxes of carbon from  $R_S$  and their temperature sensitivity vary across regions. Annual  $R_S$  rates range from several  $\text{g C m}^{-2} \text{ year}^{-1}$  in the desert and tundra to thousands of  $\text{g C m}^{-2} \text{ year}^{-1}$  in biomes such as temperate and tropic forests (Brito et al., 2009; Christiansen et al., 2012; Conant et al., 1998; Fang et al., 2012; Jiang et al., 2010; Jin et al., 2010; Lin et al., 2011; Panosso et al., 2009; Pendall et al., 2010). Even within similar biomes, the annual  $R_S$  rate varies with mean annual precipitation (MAP) and mean annual temperature (MAT). For instance, in a synthesis of  $R_S$  heterogeneity in forests across the globe, Wang et al. (2010) found that annual  $R_S$  rates from naturally regenerated forests ranged from 220 to 2,560  $\text{g C m}^{-2} \text{ year}^{-1}$  and were positively correlated with MAT. Wang et al. (2010) also found that  $R_S$  was more sensitive to MAP change (slope = 0.753) when MAP was <813 mm, but less sensitive when MAP was >813 mm (slope = 0.203). In another synthesis data from world grasslands, Wang and Fang (2009) found that annual  $R_S$  rates ranged from 52.1 to 1,004  $\text{g C m}^{-2} \text{ year}^{-1}$  in different grasslands. The  $R_S$  rates were positively correlated with MAT, but the relationship between  $R_S$  and MAP shows quadratic pattern (Wang & Fang, 2009). These differing responses to MAT and MAP create heterogeneity in  $Q_{10}$  among different biomes. The variation in  $Q_{10}$  may relate with heterogeneity in the response of  $R_S$  to temperature change among regions.

Heterogeneity in the temperature sensitivity of  $R_S$  may affect how soil carbon stocks will respond to temperature increasing. Numerous studies find that carbon stocks decrease with increasing temperature, but that decrease is regionally heterogeneous (Cramer et al., 2001; Davidson, 2016; Dorrepaal et al., 2009; Frey et al., 2013; Karhu et al., 2014; Lu et al., 2013). For example, between 1978 and 2003 soil carbon was lost at a mean rate of 0.6% per year across England and Wales due to climate change (Bellamy et al., 2005). Across North America, Europe, and Asia, Crowther et al. (2016) found that the effects of warming on soil

carbon loss depended largely on the initial soil carbon stock, with considerable soil carbon loss at high latitudes due to its high carbon stocks. However, Gestel et al. (2018) argue that this strong negative relationship between carbon loss and initial soil carbon stock no longer holds true according to the compiled data from additional warming experiments. Using organic and mineral soils from the permafrost region, Schuur et al. (2015) predicted that around 20% and 10% of soil carbon will be released after 10 years of incubation, respectively. However, other studies found no discernible trend in soil carbon stocks under temperature increasing (Liski et al., 1999; Sistla et al., 2013). Some of this heterogeneity may be linked to associated changes in primary production and resulting organic matter contributions, or to differential temperature responses of factors (e.g., aggregate protection and microbial metabolism) that control carbon loss through  $R_S$  (Conant et al., 2011). Thus, the regional heterogeneity of  $R_S$  rates and sensitivity may partially control carbon cycling and the feedbacks to climate change from regional to global scales (Bahn et al., 2008; Fang et al., 1998; Raich & Schlesinger, 1992).

Accurate modeling of  $R_S$  and carbon cycling across multiple scales is essential for predicting  $R_S$  response to climate change. Early empirical  $R_{SG}$  modeling only included coarse biome classifications. For instance, Raich and Potter (1995) analyzed the heterogeneity of  $R_S$  response to environmental factors within three biomes (moist biomes with no dramatic dry season, biomes with a distinct dry season, and wetlands) and created three biome-specific models to estimate  $R_{SG}$ . A major obstacle that causes uncertainty in regional and  $R_{SG}$  modeling is insufficient annual  $R_S$  field records with unequal distribution across localities and biomes (Raich et al., 2002). Fortunately, the number of site  $R_S$  measurements has increased substantially over the past several decades, and a continuously updated annual timescale global  $R_S$  database (SRDB) was developed (Bond-Lamberty & Thomsom, 2014). Based on the SRDB, Bond-Lamberty and Thomson (2010a, 2010b) developed boreal-, temperate-, and tropical-specific empirical models to estimate global  $R_S$  and analyze how  $R_S$  responds to global warming. Building on the updated  $R_S$  data in the SRDB are a new compendium of  $R_S$  data for Africa (Epule, 2015), as well as field  $R_S$  records from China (Song et al., 2014). Using the updated data, Zhao et al. (2017) estimated  $R_S$  for 10 biomes across the globe using artificial neural network models. These models were then united into a global  $R_S$  model that integrated the most up-to-date and complete global scale  $R_S$  data set available. Nonetheless, some biomes such as deserts, savannas, shrublands, tundras, and wetlands still have less than 100  $R_S$  records to support  $R_S$  modeling (Zhao et al., 2017). According to an analysis on how sample size affects  $R_S$  model parameterization, at least 250 data points are required to avoid added uncertainty (Jian, Steele, Thomas et al., 2018). Downscaling data from annual timescales to monthly timescales helps to resolve the insufficient  $R_S$  records problem by increasing sample size (if the measurement frequency is greater than once per year) and allowing for inclusion of measurements that do not cover a whole year. Increasing the number of measurements should help improve the accuracy of regional-scale  $R_S$  estimates and models.

The heterogeneity of  $R_S$  temperature sensitivity in different climate regions and its influence on  $R_{SG}$  in the future are not considered in previous studies. Thus, in this study, our goal was to determine how the future  $R_{SG}$  rates will change with predicted temperature scenarios, and if decreases in the sensitivity of  $R_S$  to temperature changes in some regions will offset increase in other regions enough to dampen future global fluxes. The specific objectives of this study were to (1) model the relationships between monthly  $R_S$  data and air temperature ( $T_m$ ) for eight climate regions, (2) estimate annual  $R_S$  fluxes for each region and aggregate these to the global scale, (3) predict annual  $R_{SG}$  fluxes from 1961 to 2014 and compare the temporal patterns of single versus multiple models, and (4) integrate these data into new estimates for the change in  $R_{SG}$  from 2015 to 2100 to determine how  $R_{SG}$  responds to global warming under two future temperature scenarios. Understanding how the regional-scale dynamics will affect  $R_{SG}$  rates under future temperature enhances our ability to predict changes in regional carbon stocks and global feedbacks to carbon cycling and climate change (Wieder et al., 2013).

## 2. Data and Methods

### 2.1. Data

We created a global monthly temperature and soil respiration database to support a single global-scale and climate-specific  $R_S$  models (Steele & Jian, 2018). Global, monthly air temperature between 1961 and 2014

with a spatial resolution of  $0.5^\circ$  latitude  $\times$   $0.5^\circ$  longitude was attained from the Center for Climate Research at the University of Delaware (Willmott et al., 2001). Global air temperature between 2015 and 2100 was collected from a Geophysical Fluid Dynamics Laboratory ESM 2G (GFDL-ESM 2G) model (<https://www.gfdl.noaa.gov/earth-system-model/>), for both the Representative Concentration Pathways with a possible radiative forcing value increase  $2.6 \text{ W/m}^2$  (RCP2.6) and  $8.5 \text{ W/m}^2$  (RCP8.5). We used air temperature from the GFDL-ESM 2G model because its air temperature prediction is very close to the mean of multiple CMIP5 models for both RCP 8.5 and RCP2.6 scenarios (Figure S3 in the supporting information). In addition, the GFDL-ESM 2G model has a consistent spatial resolution across the whole globe ( $2.0^\circ$  latitude  $\times$   $2.5^\circ$  longitude), and coverage of the whole study period with a monthly temporal resolution. RCP 2.6 and RCP 8.5 were selected because they represent the lowest and highest temperature future increases predicted by the Earth system models (ESMs). We compared air temperature data between 2011 and 2014 from both data sources, and the result showed that air temperature from the GFDL-ESM 2G model was highly correlated with air temperature from the Center for Climate Research at the University of Delaware ( $\text{adj } R^2 = 83.59\%$ ; data not shown). According to the IPCC AR5 report, which compared 42 climate models (Hartmann et al., 2013) and another study comparing 23 climate models from CMIP5 (Forster et al., 2013), air temperature predicted by the GFDL-ESM 2G model is close but slightly lower than the mean of multiple models.

Past estimates of the historical  $R_{SG}$  increase were based on  $R_S$  data expressed on an annual timescale (Bond-Lamberty & Thomson, 2010a, 2010b; Raich & Potter, 1995; Raich & Schlesinger, 1992; Zhao et al., 2017), but here we used monthly timescale data for two reasons. One, patterns in temperature sensitivity of  $R_S$  differ with the timescale of data. Short-term increases in temperature often cause a nonlinear response in  $R_S$  (Davidson & Janssens, 2006; Davidson et al., 2006). Likewise, comparisons of  $R_{SG}$  predicted from annual timescale and a monthly timescale data show that only monthly timescale temperature and  $R_S$  data followed a second-order-exponential change, with a threshold at  $27^\circ\text{C}$  (Jian, Steele, Thomas et al., 2018). Two, it has been recognized that the uneven spatial distribution of  $R_S$  records could bias  $R_{SG}$  estimates (Jian, Steele, Day et al., 2018; Raich & Schlesinger, 1992). To avoid the bias caused by sample size, at least 250  $R_S$  records are required to parameterize the model in each region (Jian, Steele, Thomas et al., 2018). In arid and polar regions, however, very limited measurements are available, and many of those  $R_S$  measurements were taken during warm periods rather than throughout the whole year. By using monthly timescale data, we can incorporate more  $R_S$  measurements in these regions, even though there are still data gaps for some periods. Therefore, by using monthly timescale  $R_S$  data, we increased the  $R_S$  data available to support climate-specific model parameterization and capture the second-order-exponential relationship between  $R_S$  and temperature.

We developed a Monthly Global Soil Respiration Database (MGR<sub>S</sub>D), by collecting 619 English language papers from the SRDB (Bond-Lamberty & Thomson, 2010a, 2010b). In addition, we collected 50 papers published in Chinese with English abstracts from another meta-analysis (Chen et al., 2014). Since these two meta-analyses only provide publications before 2011, additional publications were gathered via a literature search using ISI Web of Science for papers published after 2011. This generated an additional 54 papers published after 2011. We digitized most of the  $R_S$  data from figures using the software Data Thief (version III, <http://datathief.org/>).

We used the following criteria to determine if data would be included in the database. (1) The timescale of  $R_S$  measurement was monthly, daily, or subdaily. (2) If experiments exposed soil to treatments (e.g., nitrogen addition, air/soil warming, and rain/litter exclusion), only  $R_S$  measurements from control plots were included. (3)  $R_S$  collected with alkaline absorption was included only if the area of absorption was  $>6\%$  of the chamber area, and the chambers were inserted  $>5 \text{ cm}$  into the soil. Otherwise, alkaline absorption underestimates actual fluxes (Raich & Nadelhoffer, 1989). After digitization, all data were aggregated to a monthly timescale and normalized to  $\text{g C m}^{-2} \text{ day}^{-1}$ . If measurements within same location (latitude and longitude are same) and within same month of a year, the measurements were averaged to obtain a mean  $R_S$  rate. A number of ancillary data were collected. The date and location (latitude and longitude) of  $R_S$  records were directly collected from the papers. Climate classification was based on Koppen climate classification (<http://koeppen-geiger.vu-wien.ac.at/>).

Quality control was performed to guarantee the quality of the data. When all digitization was finished, we mapped sites by countries in ArcGIS (ESRI v10.2) to identify incorrect latitude or longitude information.

After site locations were checked, the climate, air temperature, monthly precipitation, and soil properties information of every site was identified based on latitude and longitude information. In addition, if the papers reported annual  $R_s$  and the monthly  $R_s$  covered the whole year, we summed them to an annual timescale and compared these with the reported annual  $R_s$  from paper or from SRDB. We assumed data were digitized correctly when the gap between the averaged  $R_s$  annual mean and paper reported or SRDB reported  $R_s$  annual mean was small (the difference is less than 5% of digitized mean). We also created  $R_s$  versus air temperature scatter plots by site to further inspect the relationship. If the  $R_s$  versus air temperature did not follow either a linear increase, a nonlinear first-order exponential, or a second-order exponential growth relationship, we double-checked the digitized data with the original paper.

After criteria and quality control, the MGR<sub>s</sub>D included records from 57 countries, including 14 monthly  $R_s$  measurements from Antarctica (Figure 1a). The  $R_s$  records of the MGR<sub>s</sub>D were dispersed from 1961 to 2014, with more data available from 1990 to 2010 (Figures 1b and 1c). More data were available from the Northern Hemisphere (12,508) than the Southern Hemisphere (974), and from temperate and boreal regions compared to tropical and polar regions (Figures 1c–1e). In the Northern Hemisphere, more  $R_s$  measurements were available during the growing season than other months (Figure 1d, the black bars), while in the Southern Hemisphere, the  $R_s$  measurements were evenly distributed among months (Figure 1d, the red bars).  $R_s$  rate in the MGR<sub>s</sub>D ranges from 0.001 to 16.201 g C m<sup>−2</sup> day<sup>−1</sup> but shows heavily right skew distribution (tail at high rate), with more data in the lower  $R_s$  rate range (Figure 1f).

## 2.2. Global Soil Respiration Modeling

We tested (1) a simple linear model, (2) a first-order (equation (1)), and (3) a second-order (equation (2)) exponential relationships between  $R_s$  and air temperature for the global scale and in each climate region. A first-order exponential model, where  $Q_{10}$  is a constant value, means that  $R_s$  responds positively to temperature increase. A second-order exponential model, where  $Q_{10}$  is negatively related with air temperature (when parameter  $b > 0$  in equation (2)).

$$R_s = F \times \exp^{(a \times T_m)}, \quad (1)$$

$$R_s = F \times \exp^{(a \times T_m - b \times T_m^2)}, \quad (2)$$

where  $F$  indicates the  $R_s$  rate when air temperature ( $T_m$ ) is zero and  $a$  indicates the increase rate of  $R_s$  with air temperature. In the second-order exponential,  $b$  donates a second-order growth of  $R_s$  with air temperature, where if  $b > 0$ , there is a threshold (i.e., optimum air temperature for  $R_s$ ) temperature in the relationship, where  $R_s$  increases with air temperature below this threshold temperature and decreases with air temperature when greater than this threshold. We parameterized both single global  $R_s$  model and models developed for each climate region, hereafter named climate-specific model, using the maximum likelihood estimation approach (nls function in R; R Development Core Team, 2014). Lastly, we calculated a threshold based on the second-order exponential model (equation (3)).

$$\text{Threshold} = \frac{-a}{2 \times b}. \quad (3)$$

## 2.3. Future and Historical $R_s$ Estimation

For each climate region and the globe, by comparing AIC and RMSE values, the best performing model was selected to estimate  $R_s$  of the study period (Table S1 and Figure 2). We predicted monthly  $R_{sG}$  from 1961 to 2014 at a spatial resolution of 0.5° longitude × 0.5° latitude. Our estimations assume it is appropriate to predict the future  $R_{sG}$  by the  $R_s$  models developed in this study based on historical  $R_s$  records. The assumption is supported by a recent analysis of  $R_s$  response to increasing temperature that found the response of  $R_s$  to temperature remained unaltered with warming, that is,  $R_s$  responded to temperature in warmed soil the same way it did in control soils (Carey et al., 2016). Annual  $R_{sG}$  from 2015 to 2100 was estimated from both a single-global model and climate-specific model, as well as air temperature estimated from the GFDL-ESM 2G model under global warming scenarios RCP2.6 and RCP8.5. We used a coarser spatial resolution (2.5° longitude × 2.0° latitude) to coincide with the air temperature data from the GFDL-ESM 2G model, which

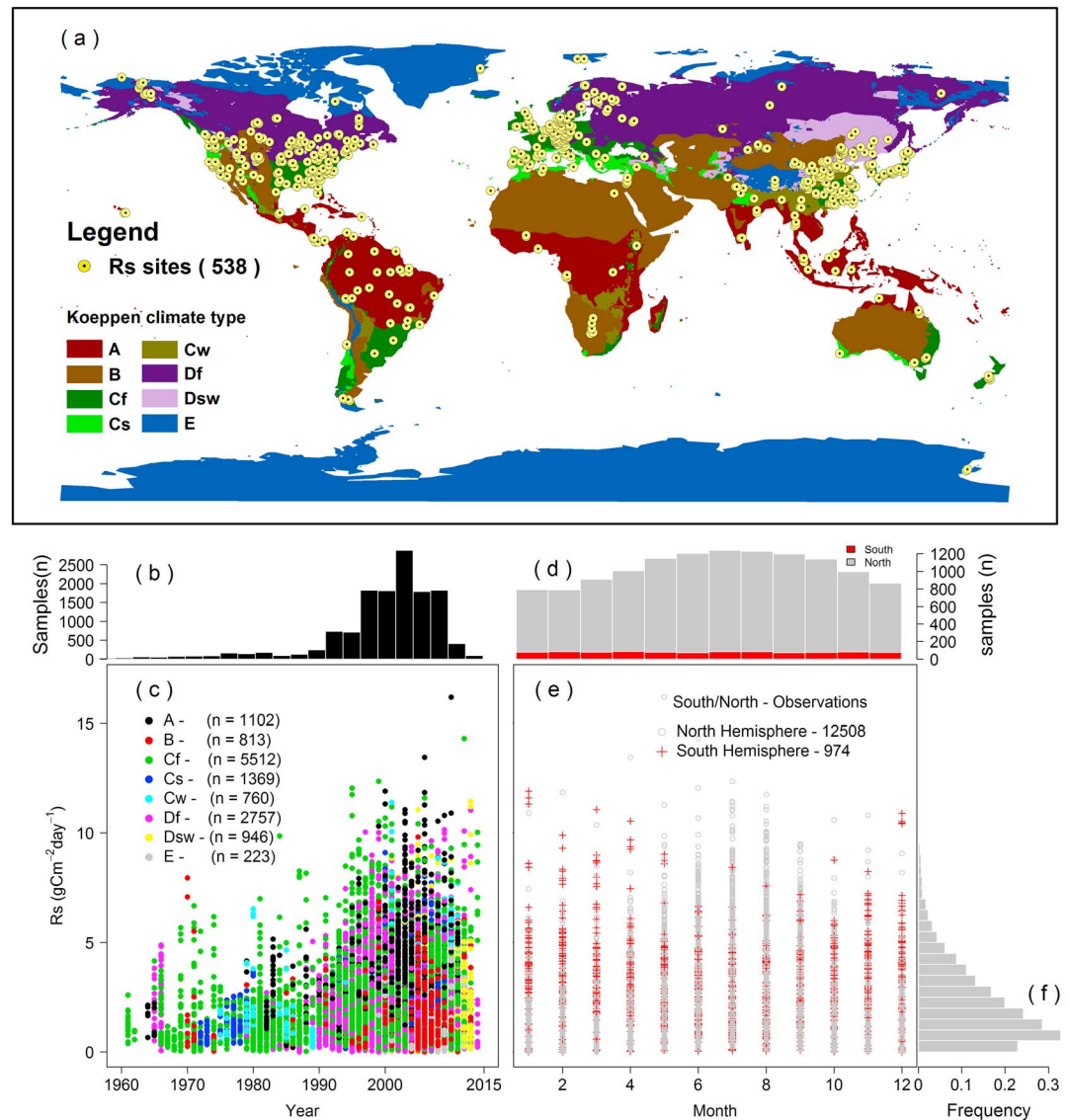


**Figure 1.** Spatial and temporal distribution of the monthly global soil respiration database (MGRSD) in tropical (A), arid (B), temperate humid (Cf), temperate summer dry (Cs), temperate winter dry (Df), boreal humid (Df), boreal summer dry or winter dry (Dsw) and polar (E) climate regions. a) Sites labeled as “Rs sites” include 538 sites in the MMGRSD. b) The frequency of soil respiration ( $R_s$ ) records from 1961 to 2014. c) The distribution of soil respiration measurements from 1961 to 2014 by different climate regions, labeled by different colors. d) The frequency of soil respiration observations distribution from January to December. e) The distribution soil respiration records from January to December in the south (red crosses) and north hemispheres (gray dots). f) The distribution of soil respiration measurements by soil respiration rate.

predicts the future air temperature. Annual  $R_{SG}$  changes from 1961 to 2014 (historical period) and from 2015 to 2100 (future) were analyzed.

To determine whether decreases in the temperature sensitivity at regional-scales might affect  $R_{SG}$  with future warming, we analyzed how the  $R_s$  anomalies were correlated with temperature anomalies.  $R_s$  or temperature anomalies are the difference between an estimate at specific year and the long-term average  $R_s$  or temperature. The anomalies present a clearer relationship of how  $R_s$  responds to temperature increasing than  $R_s$  or temperature themselves (Bond-Lamberty & Thomson, 2010a, 2010b; Hansen et al., 2010; Hashimoto et al., 2015). For easy comparison, we used mean  $R_s$  or temperature within each group as the references to calculate the  $R_s$  anomalies and

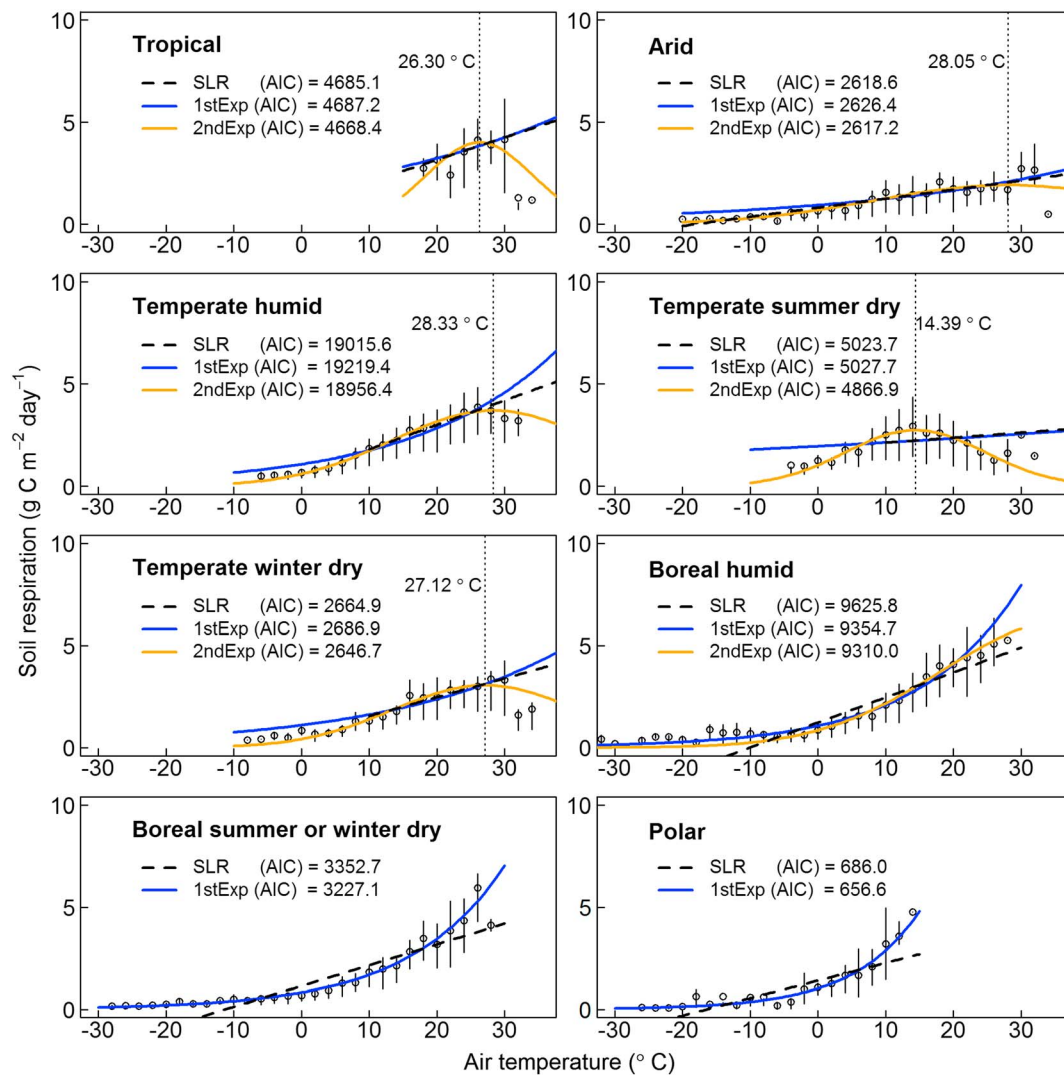


**Figure 2.** The relationship between soil respiration ( $R_s$ ) and air temperature in different climates. Hollow circles indicate median  $R_s$  and bars indicate first and third quartiles. Akaike information criterion (AIC, a measure of the relative quality of statistical models for a given set of data) values are compared to identify which model better explains soil respiration variability, smaller AIC value indicates a better model. If present, regressions are significant at  $p < 0.05$ . SLR: simple linear model, 1stExp: first-order exponential model, and 2ndExp: second-order exponential model.  $AIC = 2k - 2\ln(\hat{L})$ ,  $k$  is the number of estimated parameters in the model, and  $\hat{L}$  is the maximum value of the likelihood function for the model. Note that the AIC values can be directly acquired from R.

temperature anomalies for the historical period, RCP2.6 and RCP8.5. We analyzed how the  $R_s$  anomalies correlated with temperature anomalies for three scenarios: historically from 1961 to 2014 and both future (2015 to 2100) temperature scenarios (RCP2.6 and RCP8.5). Positive relationships indicated increases in  $R_s$  with temperature, whereas null or negative correlations indicated that  $R_s$  does not respond or decreases with temperature.

### 3. Results

#### 3.1. Regional and Global $R_s$ Estimates

The importance of air temperature as a predictor for  $R_s$  varies from region to region; air temperature explained more  $R_s$  variability in colder regions than in warmer regions (Table S1 and Figure 2). The nature of the  $R_s$  versus air temperature relationship also differed among regions. In warmer regions, the second-order models best fit temperature responses (smallest AIC value in Figure 2), while a first-order model best fit temperature response in the polar and boreal regions (Figure 2 and Table S1). The air temperature

**Table 1***The Areal Extent and Estimated Mean Annual Soil Respiration Rate ( $R_S$ ) of the Globe and for Eight Climate Regions Classified by the Koppen-Geiger Classification*

Climate Region	Number of grid cells	Area ( $10^4 \text{ km}^2$ )	Single model Mean $R_S$ rate ( $\text{g C m}^{-2} \text{ day}^{-1}$ )	Climate-specific model		Annual mean $R_S$ ( $\text{Pg C year}^{-1}$ )	Difference (Single model - Climate-specific model)
				Annual mean $R_S$ ( $\text{Pg C year}^{-1}$ )	Mean $R_S$ rate ( $\text{g C m}^{-2} \text{ day}^{-1}$ )		
A	9,746 (11.36%)	1695	3.47	21.45	3.73	23.11	−1.66 (−7.2%)
B	15,273 (17.80%)	2656	2.82	27.31	1.82	17.64	+9.67 (+54.8%)
Cf	4,868 (5.67%)	847	2.36	7.29	2.25	6.97	+0.32 (+4.6%)
Cs	1,590 (1.85%)	276	2.35	2.37	1.96	1.98	+0.39 (+19.7%)
Cw	2,046 (2.38%)	356	2.86	3.71	2.09	2.71	+1.00 (+36.9%)
Df	17,047 (19.87%)	2964	1.06	11.49	1.26	13.63	−2.14 (−15.7%)
Dsw	2,902 (3.38%)	505	1.21	2.22	1.28	2.36	−0.14 (−5.9%)
E	32,322 (37.67%)	5621	0.12	2.50	0.20	4.15	−1.65 (−39.8%)
Global	85,794	14920	1.44 (weighted)	78.34 ( $\pm 4.40$ )	1.33 (weighted)	72.55 ( $\pm 13.97$ )	+5.79 (+8.0%)

Note. Tropical (A), Arid (B), Temperate humid (Cf), Temperate summer dry (Cs), Temperate winter dry (Cw), Boreal humid (Df), Boreal summer dry or winter dry (Dsw), and Polar (E). Grid cells were  $0.5^\circ$  latitude  $\times$   $0.5^\circ$  longitude. Each cell area was calculated as  $0.173905 \times 10^4 \text{ km}^2$ . The mean  $R_S$  was weighted by region area and was averaged for each vegetation coverage from 1961 to 2014.

thresholds for  $R_S$  in warmer regions ranged from 14.4 to 28.3  $^\circ\text{C}$  (Figure 2, identified by vertical lines). A threshold was also calculated for the boreal humid region (36.98  $^\circ\text{C}$ ); however, the threshold temperature was greater than the highest monthly air temperature records from the climate data in this region, thus likely to be a spurious “threshold” and not an accurate estimate of the actual threshold in this region.

The mean annual  $R_{SG}$  from 1961 to 2014 was  $78.34 \pm 4.40 \text{ Pg C year}^{-1}$  when estimated by the single model, and  $72.55 \pm 13.97 \text{ Pg C year}^{-1}$  when estimated by the climate-specific model (Table 1). We obtained the 95% confidence interval of  $R_{SG}$  by including the 95% confidence interval of each of the model parameters (for details, please see Table S1). For example, for the single model the  $R_{SG}$  estimate is 78.34 if we use  $F = 0.77$ ,  $a = 0.11$ , and  $b = 0.002$ . The  $R_{SG}$  estimate is  $78.34 + 4.40$  if we use  $F = 0.77 + 0.024$ ,  $a = 0.11 + 0.004$ , and  $b = 0.002 + 0.0001$ . The climate-specific  $R_S$  model captured the magnitude of  $R_S$  for all climate regions and matched well with the measured data, while the single model overestimated  $R_S$  in arid climates and underestimated  $R_S$  in colder regions (Figures 3 and S1; note only  $R_S$  measurements from north hemisphere were used). The difference between  $R_S$  estimates from the single and climate-specific model at the regional scale ranged from  $-2.14$  to  $+9.67 \text{ Pg C year}^{-1}$  (Table 1 and Figure 3). The single model overestimated  $R_S$  rates in arid climates and lead to a cumulative difference of 9.67 Pg, approximately 55% of the annual flux, due to the large area of the region (Table 1). In contrast, the single model underestimated  $R_S$  by 0.14 to 2.14 Pg in boreal and polar regions (Table 1). The single model underestimated annual  $R_S$  by 1.65  $\text{Pg C year}^{-1}$ , approximately 40% of the flux in polar regions. For temperate regions, the difference between the single model and the climate-specific model was very small (Table 1).

### 3.2. Historical and Future Increase of $R_{SG}$

Historical increase of  $R_{SG}$  varied through the analysis period according to both the single and climate-specific model (Figure 4a).  $R_{SG}$  was relatively constant from 1961 to 1980, then increased rapidly at a rate of  $0.058 \text{ Pg C year}^{-1}$  from 1981 to 2000.  $R_{SG}$  then decelerated to  $0.025 \text{ Pg C year}^{-1}$  from 2001 to 2014. The damping of  $R_{SG}$  increase corresponded with the damping of global air temperature increase from 2001 to 2014 (Figure 4a). The future acceleration of  $R_{SG}$  depended on the warming scenarios. Under the RCP8.5 scenario, an approximately 3  $^\circ\text{C}$  warming, the  $R_S$  increase doubled (single model =  $+0.11 \text{ Pg C year}^{-1}$  and climate-specific model =  $+0.13 \text{ Pg C year}^{-1}$ ; Figure 4b) compared with previous decades. However, under the RCP2.6 scenario,  $R_S$  rates remained relatively constant (Figure 4b). During both the historical and future periods, the increase of global  $R_S$  estimated by climate-specific model was slightly larger than the rate of increase estimated by the single model (Figures 4a and 4b).

### 3.3. Regional $R_S$ Increase and Temperature Sensitivity

With no  $\text{CO}_2$  mitigation (RCP8.5) the increase in  $R_{SG}$  rates accelerated to twice the current rate; however, the predicted  $R_S$  rates of some regions suggest reduced sensitivity to rising temperature (Figure 5).  $R_S$  predicted

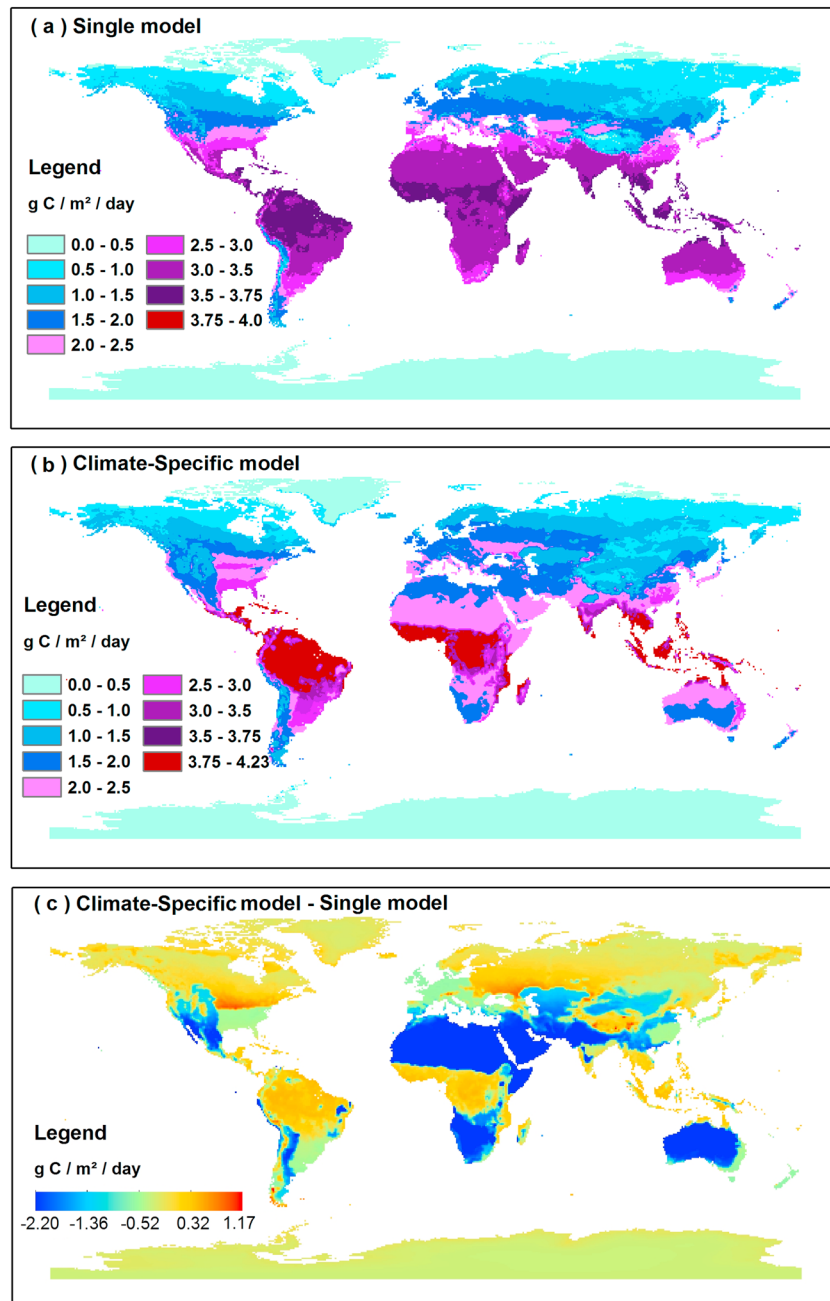


**Figure 3.** Estimated global annual soil respiration ( $\text{g C m}^{-2} \text{ year}^{-1}$ ) by global single soil respiration model parameterized based on the monthly global  $R_s$  data (panel a), by the climate-specific model parameterized based on the monthly global  $R_s$  data (panel b), and the difference between  $R_s$  estimates between the single model and climate-specific models (panel c).

by the climate-specific model was less sensitive to increases in temperature in the tropical and temperate summer dry regions, where  $R_s$  rates showed either no increase (arid) or a negative correlation with increases in temperature under RCP8.5 global warming scenario (Figures 5 and S2). In temperate, boreal, and polar regions, however, the annual  $R_s$  increased substantially as temperature increased, due to increasing sensitivity of  $R_s$  to warming (Figures 5 and S2). The single  $R_s$  model did not predict any decline in the sensitivity of  $R_s$  (Figure 5), as  $R_s$  responds to temperature positively within all climate regions and within all time periods (historical, RCP2.6, and RCP8.5).

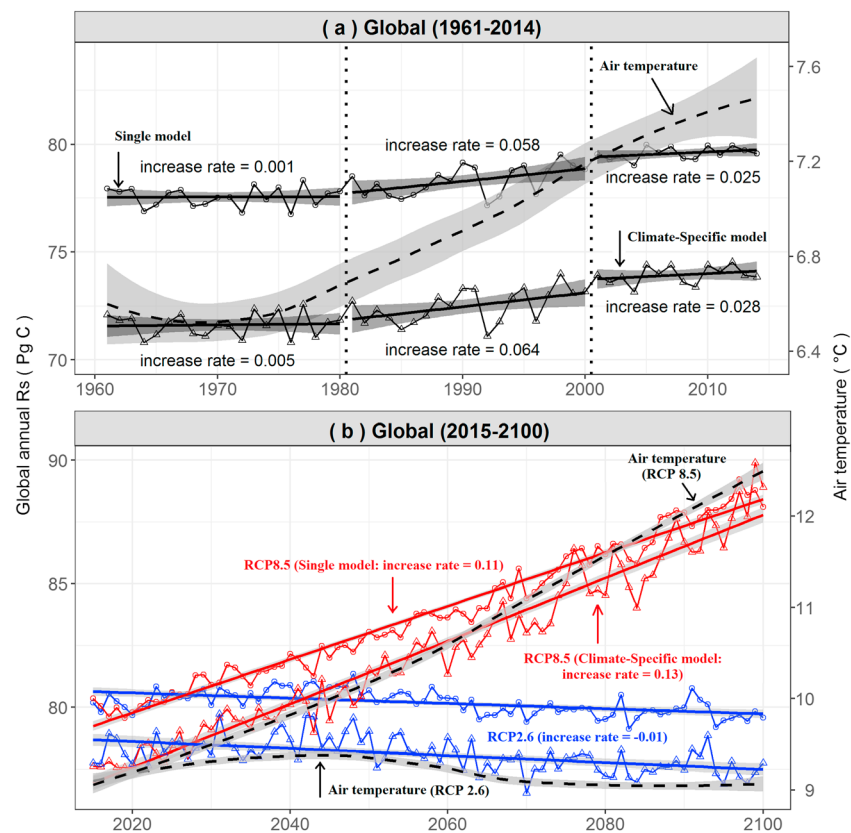


**Figure 4.** Estimated global annual soil respiration ( $R_{SG}$ ) changed from 1961 to 2014 (upper panel a) and from 2015 to 2100 (lower panel b). Future warming scenarios suggest that with mitigation of human  $CO_2$  production (RCP2.6, blue dots and lines)  $R_{SG}$  would slightly increase from 2015 to 2050 and decrease from 2050 to 2100, generally corresponding to the variations in air temperature. In contrast, unmitigated human  $CO_2$  production (RCP8.5, red dots and lines) will significantly increase future  $R_S$  rates. Circles are  $R_{SG}$  estimated by single model and triangles are  $R_{SG}$  estimated by climate-specific model. The dashed lines with confidence interval range are air temperature trends fitted by 'loess' method in R.

#### 4. Discussion

In this study, we predict that future  $R_{SG}$  rates will accelerate substantially if human  $CO_2$  emissions are not mitigated and global temperature increases by approximately  $3\text{ }^{\circ}\text{C}$  by 2100. Our historical rate of increase ( $0.04\text{ Pg C year}^{-1}$ ; Figure 4a) was consistent with prior estimates of historical  $R_{SG}$  increase (averaging  $0.04$  to  $0.10\text{ Pg C year}^{-1}$ ; Bond-Lamberty & Thomson, 2010a, 2010b; Hashimoto et al., 2015; Zhao et al., 2017) and similar between the two respiration model types we examined (Figure 4a). However, if no mitigation of human emissions occurs, the future  $R_{SG}$  rates between 2011 and 2100 are predicted to increase at higher rate, averaging  $0.11$  and  $0.13\text{ Pg C year}^{-1}$  based on the single and climate-specific model, respectively (Figure 4b). Under these conditions,  $R_{SG}$  will increase from around  $73$  to  $88\text{ Pg C year}^{-1}$  by 2100, even though the climate-specific model predicted  $R_S$  will decelerate in the arid, winter-dry and summer-dry temperates, and tropical climates (Figure 5).

When comparing  $R_{SG}$  estimated by the single-global and climate-specific model, we found that  $R_{SG}$  during the historical period (1961 to 2014) estimated from the single model (mean with 95% confidence interval:  $78.34 \pm 4.40$ ) was around  $6\text{ Pg C}$  larger than that estimated by the region-specific model ( $72.55 \pm 13.97\text{ Pg C year}^{-1}$ ). The estimates were consistent with previous estimates based on monthly  $R_S$  data (Jian, Steele, Thomas et al., 2018) but lower than previous estimates based on annual  $R_S$  data (Bond-Lamberty & Thomson, 2010a, 2010b; Hashimoto et al., 2015; Zhao et al., 2017). The differing results from the single model and the climate-specific model were likely caused by the regional heterogeneity of  $R_S$  response to temperature change (Figure 2). For instance, a threshold at  $14.39\text{ }^{\circ}\text{C}$  was detected in the temperate

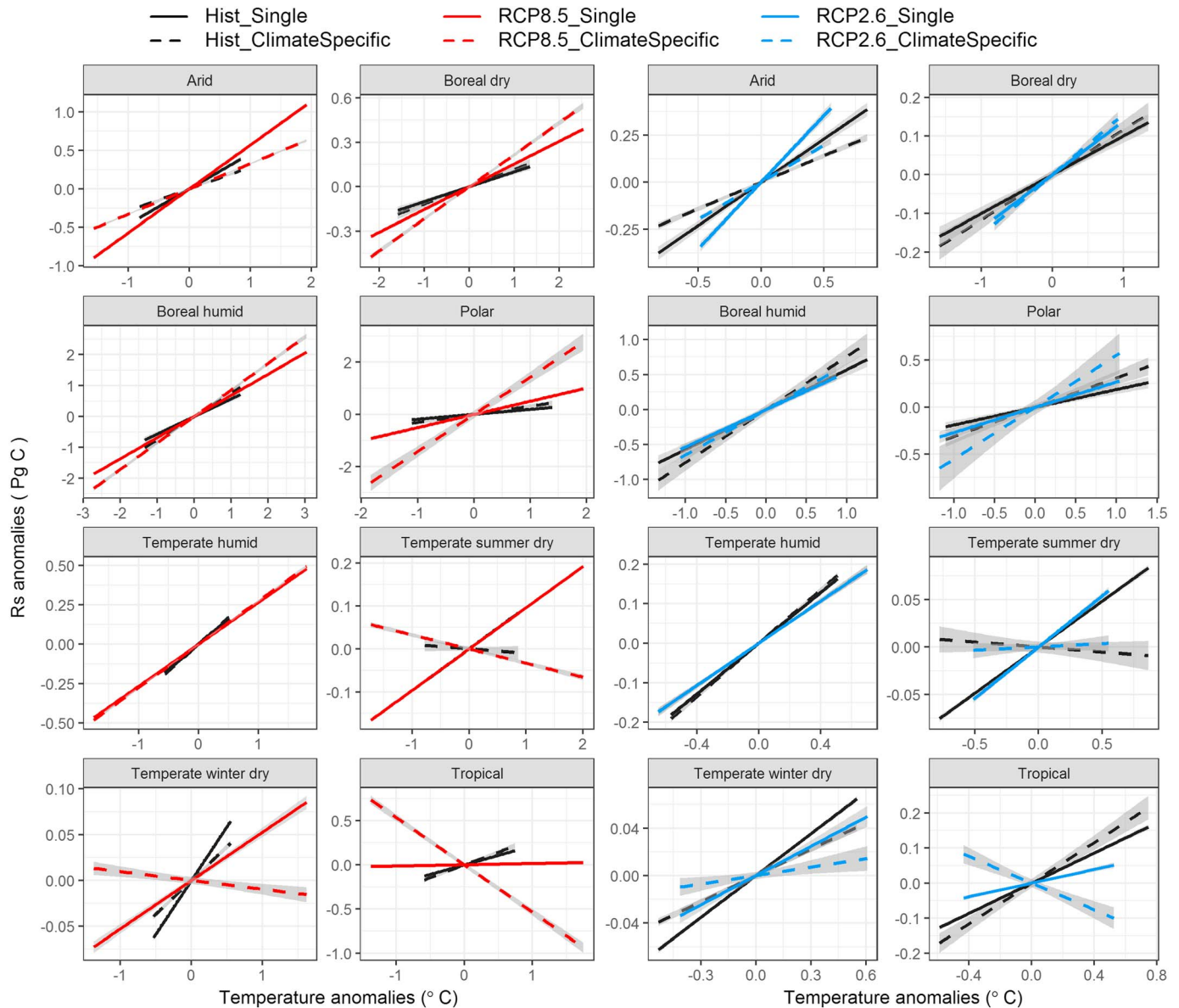


**Figure 5.** Relationship between the estimated annual soil respiration ( $R_s$ ) anomalies and temperature anomalies from 1961 to 2014 (black lines) and from 2015 to 2100 under unmitigated human  $\text{CO}_2$  production scenario (RCP8.5, red lines) and mitigated human  $\text{CO}_2$  production (RCP2.6, blue lines). Solid lines represent results from the single model, while dashed lines are results from climate climate-specific model. From 2015 to 2100 under the RCP8.5 scenario,  $R_s$  decreased in sensitivity in tropical, temperate summer-dry and temperate winter-dry climates; however, this was only detected by the climate-specific model. In boreal and polar climates, however,  $R_s$  was even more sensitive to temperature in the future under RCP8.5 compared to the historical period. Note that x-axis and y-axis differ from panel to panel.

summer-dry region by the climate-specific model; however, in the single-global model the threshold was  $27.50^\circ\text{C}$  (Figure 2). Thus, when over  $14.39^\circ\text{C}$ ,  $R_s$  was negatively correlated with temperature increase under climate-specific model, but the single model still predicted positive response in temperate summer dry region until over  $27.50^\circ\text{C}$ . The difference likely caused the modest increase in global estimates by the single model.

The difference between predictions from the single-global model and using climate-specific model highlights the need to account for regional heterogeneity in the response of  $R_s$  to temperature when studying the effects of warming on soil-carbon dynamics in future. However, climate-specific model require sufficient data coverage for each region. For example, polar and arid regions make up 37.67% and 17.80%,

respectively, of total area across globe; however, only 223 and 813 records were available from these region, accounting for 1.65% and 6.03% of total records from MGR<sub>5</sub>D. The lack of data in these regions contributes some uncertainty, and more measurements from these regions would be valuable to R<sub>SG</sub> estimates (Table 1 and Figure 3).

Though we observed that a decrease in temperature sensitivity caused R<sub>5</sub> to decrease in some large regions, the climate-specific model predicted R<sub>5</sub> was more sensitive to temperature increases in colder regions and increased R<sub>5</sub> from the boreal and polar regions overwhelmed future R<sub>SG</sub> rates (Figures S2 and 5). The predicted increase in R<sub>5</sub> from the boreal and polar regions may have substantial effects on losses of carbon stocks in those regions. The temperature of colder regions is increasing at higher rate compared to the rest of the globe, and almost 1,700 Pg of organic carbon is stored in the permafrost (Tarnocai et al., 2009). A recent meta-analysis compared total soil carbon under warming and ambient conditions across Eurasia and North America found that warming stimulated carbon losses from soil to the atmosphere regardless of how many years the full soil carbon response to warming is realized, but with a very large range of uncertainty (Crowther et al., 2016). Given the larger increases in rate observed in this study, the loss of soil carbon stocks may be towards the upper end (around 200 Pg C) of the uncertainty bounds if human emissions are not limited (Crowther et al., 2016), mainly driven by carbon losses in colder climates. An increase in primary production carbon may offset losses from soil respiration, as a recent study found that the rate of net biome productivity (which is the difference between net primary production and autotrophic respiration) has significantly accelerated during the warming hiatus (1998–2012; Ballantyne et al., 2017). However, substantial uncertainty still exists in the response of primary productivity to CO<sub>2</sub> fertilization (Korner et al., 2005; Norby et al., 2005, 2010) and global warming induced drought at regional and global scales (Yuan et al., 2016; Zhao & Running, 2010).

In this study, we developed models based on historical data to forecast future trends, an approach that incorporated several assumptions regarding the response of R<sub>SG</sub> to increasing temperature. First, predicting future R<sub>SG</sub> from models developed with historical R<sub>5</sub> data assumes that the R<sub>5</sub> response to temperature will follow the same relationship despite warming climates. This precondition is supported by a recent analysis of soil warming data (Carey et al., 2016); however, warming experiments can alter factors so that they are not fully representative of future conditions (Conant et al., 2011). Second, we assumed that the limited range and availability of R<sub>5</sub> data from the cold regions was sufficient to represent the R<sub>5</sub> response to temperature in a critical region. Data from boreal and polar regions does not show a threshold and the future R<sub>5</sub> predictions also do not decline within the 3 °C increase predicted by RCP8.5. While it is possible that with continued warm R<sub>5</sub> in the polar and boreal regions will reach threshold temperature some time, with a 3 °C increase, the temperature is still much below an anticipated threshold (27 °C). Therefore, we believe our predictions for the next 82 years based on this assumption are valid estimates. Given the critical contribution of cold regions in global carbon fluxes, more R<sub>5</sub> measurements will be needed to verify or modify existing models as temperature begin to reach threshold values in the future. Third, we assumed that air temperature is, and will continue to be, the major factor influencing R<sub>5</sub> under global warming and omit the potential influence of changing precipitation patterns and vegetation. We acknowledge that these factors may affect future R<sub>SG</sub> rates. For example, extreme droughts are more sensitive to climate change and large-scale droughts have been shown reduce regional net primary production (Yan et al., 2015; Zhao & Running, 2010). We omit these influences in our models and estimates because, one, current climate models are less confident on how precipitation and vegetation will change under global warming and, two, we lack reliable data to analyze how precipitation and vegetation change in the future (IPCC, 2007). A more intensive investigation of precipitation and vegetation affect R<sub>5</sub> under global warming is beyond the scope of this study.

ESMs play a critical role in understanding the mechanisms of soil respiration, as well as projections future climate change. The soil submodels of the ESMs use simple abiotic relationships to predict how soil carbon will respond to warming and simulate heterotrophic respiration (Arora et al., 2013; Wieder et al., 2013). R<sub>5</sub> comes from both heterotrophic respiration (microbial respiration) and autotrophic respiration (root respiration), but current global R<sub>5</sub> models do not separate R<sub>5</sub> into these two components. Estimates of heterotrophic respiration cannot be directly compared with R<sub>5</sub> estimates, as each component of R<sub>5</sub> should respond differently to climate change because plant communities and microbial communities will not respond in the same manner (Bond-Lamberty et al., 2004). In addition, the CMIP5 models have not accurately captured the current warming hiatus (1998–2014), which has led to an overestimation of ecosystem respiration comparing with

observations (Ballantyne et al., 2017). An empirical model based on soil moisture and soil temperature data better estimated the reduced ecosystem respiration during warming hiatus (Ballantyne et al., 2017). A similar conclusion was reached by Lynch et al. (2017), whom found that heterotrophic respiration of 25 models from CMIP5 are significantly higher than heterotrophic respiration predicted by a statistical model. Even though it requires several key conditions (e.g., broad participation of countries and sectors to reduce greenhouse gas emissions, optimistic assumptions on mitigation potential, and protect forests) to reach 2.6 W/m<sup>2</sup> radiative forcing levels by 2100 (van Vuuren et al., 2011), one advantage of using RCP2.6 in this study was that it provided an opportunity to approximate R<sub>SG</sub> dynamics under a warming hiatus situation, which are not well captured by the current ESMs.

One critical point in this study is the existence of a threshold in the relationship between R<sub>S</sub> and temperature, where R<sub>S</sub> peaks and then declines as temperature rises. Theoretically, thermal acclimation should be a common property for all organisms, including decomposers. Respiratory enzymes bind substrates under initial conformation, then transport to the reaction place where the enzymes change their conformation and release the substrates (Crowther & Bradford, 2013). Microbial communities adapted to warming conditions are less sensitive to temperature change than communities adapted at low temperature (Bradford et al., 2008; Crowther & Bradford, 2013). Currently, estimates of changes in R<sub>S</sub> from temperature increase are mostly from incubation studies or field warming experiments (Carey et al., 2016; Hamdi et al., 2013). Presuming microbial populations adapt, or there are shifts in the microbial communities in response to shifts in the environment, these threshold temperature may change over the timescales of many decades as opposed to incubation or warming studies (Bradford et al., 2016). Also, the proportion of microbial activity that is explained by the thermal adaptation could potentially explained by labile carbon depletion or explained by nitrogen limit (Cramer et al., 2001; Dorrepaal et al., 2009; Frey et al., 2013). Thus, current ESMs do not incorporate any/many of the feedback loops inherent in a warming planet. Our study analyzed the R<sub>SG</sub> dynamics under long term global warming based on simple, data-oriented R<sub>S</sub> models, and the results can be used to bridge a gap between process models and field data.

At present, terrestrial ecosystems remove around 1.7 Pg C from atmosphere each year, which help mitigate global warming (Le Quéré et al., 2013). Whether terrestrial ecosystems can remain as carbon sinks depends partially on how soil carbon responds to global warming. Our results indicate that without human mitigation of CO<sub>2</sub>, even though the temperature sensitivity of R<sub>S</sub> will decrease in some climates, we can expect even large R<sub>S</sub> fluxes at the global scale that may reduce the ecosystem's capacity to act as a carbon sink.

## 5. Conclusions

In this study, we determined that one, the future R<sub>SG</sub> rates will accelerate substantially with predicted increases temperature if no CO<sub>2</sub> mitigation occurs, and two, a decrease in the temperature sensitivity of R<sub>S</sub> of some warm regions will be offset by the increase of R<sub>S</sub> in colder regions. Each climate type had a distinct relationship between R<sub>S</sub> and air temperature that influenced how R<sub>S</sub> responded to future temperature increase and highlighted the importance of accounting for regional heterogeneity in global scale modeling and estimates. This study provides further evidence that R<sub>S</sub> deceleration could occur at large spatial scales; unfortunately, this decreasing in temperature sensitivity of R<sub>S</sub> will likely not be strong enough to suppress the surge in soil respiration rates if global temperature is allowed to rise by 3 °C.

## Acknowledgments

This study was supported by Hatch Grant (funding: 160060) and VT Open Access Subvention Fund (OASF, funding: 124166). All data used for this study can be found at <https://data.lib.vt.edu/collections/ns0646000>.

## References

- Arora, V. K., Boer, G. J., Friedlingstein, P., Eby, M., Jones, C. D., Christian, J. R., Bonan, G., et al. (2013). Carbon-concentration and carbon-climate feedbacks in CMIP5 earth system models. *Journal of Climate*, 26(15), 5289–5314. <https://doi.org/10.1175/JCLI-D-12-00494.1>
- Bahn, M., Rodeghiero, M., Anderson-Dunn, M., Dore, S., Gimeno, C., Drösler, M., Williams, M., et al. (2008). Soil respiration in European Grasslands in relation to climate and assimilate supply. *Ecosystems (New York, N.Y.)*, 11(8), 1352–1367. <https://doi.org/10.1007/s10021-008-9198-0>
- Ballantyne, A., Smith, W., Anderegg, W., Kauppi, P., Sarmiento, J., Tans, P., Shevliakova, E., et al. (2017). The warming hiatus due to reduced respiration. *Nature Climate Change*, 7(2), 148. <https://doi.org/10.1038/NCLIMATE3204>
- Bellamy, P. H., Loveland, P. J., Bradley, R. I., Lark, R. M., & Kirk, G. J. D. (2005). Carbon losses from all soils across England and Wales 1978–2003. *Nature*, 437(7056), 245–248. <https://doi.org/10.1038/nature04038>
- Bond-Lamberty, B., & Thomson, A. (2010a). A global database of soil respiration data. *Biogeosciences*, 7(6), 1915–1926. <https://doi.org/10.5194/bg-7-1915-2010>
- Bond-Lamberty, B., & Thomson, A. (2010b). Temperature-associated increases in the global soil respiration record. *Nature*, 464(7288), 579–582. <https://doi.org/10.1038/nature08930>

- Bond-Lamberty, B., & Thomsom, A. (2014). A global database of soil respiration data, Version 3.0. ORNL Distributed Active Archive Center. <https://doi.org/10.3334/ormlaoc/1235>
- Bond-Lamberty, B., Wang, C., & Gower, S. T. (2004). A global relationship between the heterotrophic and autotrophic components of soil respiration? *Global Change Biology*, 10(10), 1756–1766. <https://doi.org/10.1111/j.1365-2486.2004.00816.x>
- Bradford, M. A., Davies, C. A., Frey, S. D., Maddox, T. R., Melillo, J. M., Mohan, J. E., Reynolds, J. F., et al. (2008). Thermal adaptation of soil microbial respiration to elevated temperature. *Ecology Letters*, 11(12), 1316–1327. <https://doi.org/10.1111/j.1461-0248.2008.01251.x>
- Bradford, M. A., Wieder, W. R., Bonan, G. B., Fierer, N., Raymond, P. A., & Crowther, T. W. (2016). Managing uncertainty in soil carbon feedbacks to climate change. *Nature Climate Change*, 6(8), 751–758. <https://doi.org/10.1038/nclimate3071>
- Brito, L. D. F., Pereira, G. T., & Menezes, Z. (2009). Soil CO<sub>2</sub> emission of sugarcane fields as affected by topography. *Sci. Agric. (Piracicaba, Braz.)*, 66(February), 77–83. <https://doi.org/10.1590/S0103-90162009000100011>
- Carey, J. C., Tang, J., Templer, P. H., Kroeger, K. D., Crowther, T. W., Burton, A. J., et al. (2016). Temperature response of soil respiration largely unaltered with experimental warming. *Proceedings of the National Academy of Sciences*, 113(48), 13793–13802.
- Chen, S., Zou, J., Hu, Z., Chen, H., & Lu, Y. (2014). Global annual soil respiration in relation to climate, soil properties and vegetation characteristics: Summary of available data. *Agricultural and Forest Meteorology*, 198–199, 335–346. <https://doi.org/10.1016/j.agrformet.2014.08.020>
- Christiansen, C. T., Svendsen, S. H., Schmidt, N. M., & Michelsen, A. (2012). High arctic heath soil respiration and biogeochemical dynamics during summer and autumn freeze-in - effects of long-term enhanced water and nutrient supply. *Global Change Biology*, 18(10), 3224–3236. <https://doi.org/10.1111/j.1365-2486.2012.02770.x>
- Conant, R. T., Klopatek, J. M., Malin, R. C., & Klopatek, C. C. (1998). Carbon pools and fluxes along an environmental gradient in northern Arizona. *Biogeochemistry*, 43(1), 43–61. <https://doi.org/10.1023/A:1006004110637>
- Conant, R. T., Ryan, M. G., Agren, G. I., Birge, H. E., Davidson, E. A., Eliasson, P. E., Peter, E., et al. (2011). Temperature and soil organic matter decomposition rates—Synthesis of current knowledge and a way forward. *Global Change Biology*, 17(11), 3392–3404. <https://doi.org/10.1111/j.1365-2486.2011.02496.x>
- Cramer, W., Bondeau, A., Woodward, F. I., Prentice, I. C., Betts, R. A., Brovkin, V., Cox, P. M., et al. (2001). Global response of terrestrial ecosystem structure and function to CO<sub>2</sub> and climate change: Results from six dynamic global vegetation models. *Global Change Biology*, 7(4), 357–373. <https://doi.org/10.1046/j.1365-2486.2001.00383.x>
- Crowther, T., Todd-Brown, K., Rowe, C., Wieder, W., Carey, J., Machmuller, M., et al. (2016). Quantifying global soil C losses in response to warming. *Nature*. <https://doi.org/10.1038/nature20150>, 540(7631), 104–108.
- Crowther, T. W., & Bradford, M. A. (2013). Thermal acclimation in widespread heterotrophic soil microbes. *Ecology Letters*, 16(4), 469–477. <https://doi.org/10.1111/ele.12069>
- Davidson, E. A. (2016). Biogeochemistry: Projections of the soil-carbon deficit. *Nature*, 540(7631), 47–48. <https://doi.org/10.1038/540047a>
- Davidson, E. A., & Janssens, I. A. (2006). Temperature sensitivity of soil carbon decomposition and feedbacks to climate change. *Nature*, 440(March), 165–173. <https://doi.org/10.1038/nature04514>
- Davidson, E. A., Janssens, I. A., & Lou, Y. (2006). On the variability of respiration in terrestrial ecosystems: Moving beyond Q<sub>10</sub>. *Global Change Biology*, 12(2), 154–164. <https://doi.org/10.1111/j.1365-2486.2005.01065.x>
- Dorrepaal, E., Toet, S., van Logtestijn, R. S. P., Swart, E., van de Weg, M. J., Callaghan, T. V., et al. (2009). Carbon respiration from subsurface peat accelerated by climate warming in the subarctic. *Nature*, 460(7255), 616–619. <https://doi.org/10.1038/nature08216>
- Epule, T. (2015). A new compendium of soil respiration data for Africa. *Challenges*, 6(1), 88–97. <https://doi.org/10.3390/challe6010088>
- Fang, C., Moncrieff, J. B., Gholz, H. L., & Clark, K. L. (1998). Soil CO<sub>2</sub> efflux and its spatial variation in a Florida slash pine plantation. *Plant and Soil*, 205, 135–146.
- Fang, H., Cheng, S., Yu, G., Zheng, J., Zhang, P., Xu, M., Li, Y., et al. (2012). Responses of CO<sub>2</sub> efflux from an alpine meadow soil on the Qinghai Tibetan Plateau to multi-form and low-level N addition. *Plant and Soil*, 351(1–2), 177–190. <https://doi.org/10.1007/s11104-011-0942-4>
- Forster, P. M., Andrews, T., Good, P., Gregory, J. M., Jackson, L. S., & Zelinka, M. (2013). Evaluating adjusted forcing and model spread for historical and future scenarios in the CMIP5 generation of climate models. *Journal of Geophysical Research: Atmospheres*, 118, 1139–1150. <https://doi.org/10.1002/jgrd.50174>
- Frey, S. D., Lee, J., Melillo, J. M., & Six, J. (2013). The temperature response of soil microbial efficiency and its feedback to climate. *Nature Climate Change*, 3(4), 395–398. <https://doi.org/10.1038/nclimate1796>
- Gestel, N., Van Shi, Z., Van Groenigen, K. J., Van Osenberg, C. W., Andresen, L. C., Dukes, J. S., et al. (2018). Brief communications arising predicting soil carbon loss with warming. *Nature Publishing Group*, 554(7693), E4–E5. <https://doi.org/10.1038/nature25745>
- Hamdi, S., Moyano, F., Sall, S., Bernoux, M., & Chevallier, T. (2013). Synthesis analysis of the temperature sensitivity of soil respiration from laboratory studies in relation to incubation methods and soil conditions. *Soil Biology and Biochemistry*, 58, 115–126. <https://doi.org/10.1016/j.soilbio.2012.11.012>
- Hansen, J., Ruedy, R., Sato, M., & Lo, K. (2010). Global surface temperature change. *Rev. Geophys.*, 48, RG4004. <https://doi.org/10.1029/2010RG000345.1>
- Hartmann, D. L., Klein Tank, A. M. G., Rusticucci, M., Alexander, L. V., Brönnimann, S., Charabi, Y. A. R., et al. (2013). Observations: Atmosphere and surface. In *Climate Change 2013 the Physical Science Basis: Working group I contribution to the Fifth Assessment Report of the Intergovernmental Panel on Climate Change* (pp. 159–254). Cambridge, UK: Cambridge University Press. <https://doi.org/10.1017/CBO9781107415324.008>
- Hashimoto, S., Carvalhais, N., Ito, A., Migliavacca, M., Nishina, K., & Reichstein, M. (2015). Global spatiotemporal distribution of soil respiration modeled using a global database. *Biogeosciences Discussions*, 12(5), 4331–4364. <https://doi.org/10.5194/bgd-12-4331-2015>
- Hursh, A., Ballantyne, A., Cooper, L., Maneta, M., Kimball, J., & Watts, J. (2017). The sensitivity of soil respiration to soil temperature, moisture, and carbon supply at the global scale. *Global Change Biology*, 23(5), 2090–2103. <https://doi.org/10.1111/gcb.13489>
- IPCC (2007). In S. Solomon, D. Qin, M. Manning, Z. Chen, M. Marquis, K. B. Averyt, et al. (Eds.), *Climate change 2007: The physical science basis. Contribution of working group I to the Fourth Assessment Report of the Intergovernmental Panel on Climate Change*. Cambridge, United Kingdom and New York, NY, USA: Cambridge University Press. <https://doi.org/10.1017/CBO9780511546013>
- Janssens, I. A., Lankreijer, H., Matteucci, G., Kowalski, A. S., Buchmann, N., Epron, D., Pilegaard, K., et al. (2001). Productivity overshadows temperature in determining soil and ecosystem respiration across European forests. *Global Change Biology*, 7(3), 269–278. <https://doi.org/10.1046/j.1365-2486.2001.00412.x>
- Jian, J., Steele, M. K., Day, S. D., Quinn Thomas, R., & Hodges, S. C. (2018). Measurement strategies to account for soil respiration temporal heterogeneity across diverse regions. *Soil Biology and Biochemistry*, 125(July), 167–177. <https://doi.org/10.1016/j.soilbio.2018.07.003>

- Jian, J., Steele, M. K., Thomas, R. Q., Day, S. D., & Hodges, S. C. (2018). Constraining estimates of global soil respiration by quantifying sources of variability. *Global Change Biology*, 24, 4143–4159. <https://doi.org/10.1111/gcb.14301>
- Jiang, C., Yu, G., Cao, G., Li, Y., Zhang, S., & Fang, H. (2010). CO<sub>2</sub> flux estimation by different regression methods from an Alpine Meadow on the Qinghai-Tibetan Plateau. *Advances in Atmospheric Sciences*, 27(6), 1372–1379. <https://doi.org/10.1007/s00376-010-9218-9>
- Jin, Z., Dong, Y. S., Qi, Y. C., & An, Z. S. (2010). Soil respiration and net primary productivity in perennial grass and desert shrub ecosystems at the Ordos Plateau of Inner Mongolia, China. *Journal of Arid Environments*, 74(10), 1248–1256. <https://doi.org/10.1016/j.jaridenv.2010.05.018>
- Karhu, K., Auffret, M. D., Dungait, J. A. J., Hopkins, D. W., Prosser, J. I., Singh, B. K., Subke, J. A., et al. (2014). Temperature sensitivity of soil respiration rates enhanced by microbial community response. *Nature*, 513(7516), 81–84. <https://doi.org/10.1038/nature13604>
- Korner, C., Asshoff, R., Bignucolo, O., Hattenschwiler, S., Keel, S. G., Pelaez-Riedl, S., Pepin, S., et al. (2005). Carbon flux and growth in mature deciduous forest trees exposed to elevated CO<sub>2</sub>. *Science*, 309(5739), 1360–1362. <https://doi.org/10.1126/science.1113977>
- Le Quéré, C., Andres, R. J., Boden, T., Conway, T., Houghton, R. A., House, J. I., et al. (2013). The global carbon budget 1959–2011. *Earth System Science Data*, 5(1), 165–185. <https://doi.org/10.5194/essd-5-165-2013>
- Lellei-Kovács, E., Kovács-Láng, E., Botta-Dukát, Z., Kalapos, T., Emmett, B., & Beier, C. (2011). Thresholds and interactive effects of soil moisture on the temperature response of soil respiration. *European Journal of Soil Biology*, 47(4), 247–255.
- Lin, X., Zhang, Z., Wang, S., Hu, Y., Xu, G., Luo, C., Chang, X., et al. (2011). Response of ecosystem respiration to warming and grazing during the growing seasons in the alpine meadow on the Tibetan plateau. *Agricultural and Forest Meteorology*, 151(7), 792–802. <https://doi.org/10.1016/j.agrformet.2011.01.009>
- Liski, J., Ilvesniemi, H., & Westman, C. J. (1999). CO<sub>2</sub> emissions from soil in response to climatic warming are overestimated: The decomposition of old soil organic matter is tolerant of temperature. *Ambio*, 28(2), 171–174. <https://doi.org/10.2307/4314871>
- Lloyd, J., & Taylor, J. A. (1994). On the temperature dependence of soil respiration. *Functional Ecology*, 8(3), 315–323. Retrieved from <http://www.jstor.org/stable/2389824>
- Lu, M., Zhou, X., Yang, Q., Li, H., Luo, Y., Fang, C., Chen, J., et al. (2013). Responses of ecosystem carbon cycle to experimental warming: A meta-analysis. *Ecology*, 94(3), 726–738. <https://doi.org/10.1890/12-0279.1>
- Luo, Y., Wan, S., Hui, D., & Wallace, L. L. (2001). Acclimatization of soil respiration to warming in a tall grass prairie. *Nature*, 413(October), 622–625. <https://doi.org/10.1038/35098065>
- Norby, R. J., DeLucia, E. H., Gielen, B., Calfapietra, C., Giardina, C. P., King, J. S., Ledford, J., et al. (2005). Forest response to elevated CO<sub>2</sub> is conserved across a broad range of productivity. *Proceedings of the National Academy of Sciences*, 102(50), 18052–18056. <https://doi.org/10.1073/pnas.0509478102>
- Norby, R. J., Warren, J. M., Iversen, C. M., Medlyn, B. E., & McMurtrie, R. E. (2010). CO<sub>2</sub> enhancement of forest productivity constrained by limited nitrogen availability. *Proceedings of the National Academy of Sciences of the United States of America*, 107(45), 19368–19373. <https://doi.org/10.1073/pnas.1006463107>
- Panosso, A. R., Marques, J., Pereira, G. T., & La Scala, N. (2009). Spatial and temporal variability of soil CO<sub>2</sub> emission in a sugarcane area under green and slash-and-burn managements. *Soil and Tillage Research*, 105(2), 275–282. <https://doi.org/10.1016/j.still.2009.09.008>
- Parker, L. W., Miller, J., Steinberger, Y., & Whitford, W. G. (1983). Soil respiration in a Chihuahuan Desert Rangeland. *Soil Biology & Biochemistry*, 15(3), 303–309.
- Pendall, E., Schwendenmann, L., Rahn, T., Miller, J. B., Tans, P. P., & White, J. W. C. (2010). Land use and season affect fluxes of CO<sub>2</sub>, CH<sub>4</sub>, CO, N<sub>2</sub>O and H<sub>2</sub> and isotopic source signatures in Panama: Evidence from nocturnal boundary layer profiles. *Global Change Biology*, 16(10), 2721–2736. <https://doi.org/10.1111/j.1365-2486.2010.02199.x>
- R Development Core Team (2014). *R: A language and environment for statistical computing*, (p. 2013). Vienna, Austria: R Foundation for Statistical Computing.
- Raich, J. W., & Nadelhoffer, K. J. (1989). Belowground carbon allocation in forest ecosystems: Global trends. *Ecological Society of America*, 70(5), 1346–1354. Retrieved from <http://www.jstor.org/stable/1938194>
- Raich, J. W., & Potter, C. S. (1995). Global patterns of carbon dioxide emissions from soils. *Global Biogeochemical Cycles*, 9(1), 23–36. <https://doi.org/10.1029/94GB02723>
- Raich, J. W., Potter, C. S., & Bhagawati, D. (2002). Interannual variability in global soil respiration, 1980–94. *Global Change Biology*, 8(8), 800–812. <https://doi.org/10.1046/j.1365-2486.2002.00511.x>
- Raich, J. W., & Schlesinger, W. H. (1992). The global carbon dioxide flux in soil respiration and its relationship to vegetation and climate. *Tellus*, 44 B(2), 81–99. <https://doi.org/10.1034/j.1600-0889.1992.t01-1-00001.x>
- Schuur, E. A. G., McGuire, A. D., Schädel, C., Grosse, G., Harden, J. W., Hayes, D. J., Hugelius, G., et al. (2015). Climate change and the permafrost carbon feedback. *Nature*, 520(7546), 171–179. <https://doi.org/10.1038/nature14338>
- Sistla, S. a., Moore, J. C., Simpson, R. T., Gough, L., Shaver, G. R., & Schimel, J. P. (2013). Long-term warming restructures Arctic tundra without changing net soil carbon storage. *Nature*, 497(7451), 615–618. <https://doi.org/10.1038/nature12129>
- Song, X., Peng, C., Zhao, Z., Zhang, Z., Guo, B., Wang, W., Jiang, H., et al. (2014). Quantification of soil respiration in forest ecosystems across China. *Atmospheric Environment*, 94, 546–551. <https://doi.org/10.1016/j.atmosenv.2014.05.071>
- Steele, M. K., & Jian, J. (2018). *Monthly Global Soil Respiration Database (MGRSD)*. Virginia, U.S.A: Blacksburg: VTechData. <https://doi.org/doi:10.7294/W400008X>
- Tarnocai, C., Canadell, J. G., Schuur, E. A. G., Kuhry, P., Mazhitova, G., & Zimov, S. (2009). Soil organic carbon pools in the northern circumpolar permafrost region. *Global Biogeochemical Cycles*, 23, D07307. <https://doi.org/10.1029/2008GB003327>
- Trumbore, S. (2006). Carbon respired by terrestrial ecosystems—recent progress and challenges. *Global Change Biology*, 2, 141–153. <https://doi.org/10.1111/j.1365-2486.2005.01067.x>
- van Vuuren, D. P., Stehfest, E., den Elzen, M. G. J., Kram, T., van Vliet, J., Deetman, S., Isaac, M., et al. (2011). RCP2.6: Exploring the possibility to keep global mean temperature increase below 2 °C. *Climatic Change*, 109(1–2), 95–116. <https://doi.org/10.1007/s10584-011-0152-3>
- Wang, W., Chen, W., & Wang, S. (2010). Forest soil respiration and its heterotrophic and autotrophic components: Global patterns and responses to temperature and precipitation. *Soil Biology and Biochemistry*, 42(8), 1236–1244. <https://doi.org/10.1016/j.soilbio.2010.04.013>
- Wang, W., & Fang, J. (2009). Soil respiration and human effects on global grasslands. *Global and Planetary Change*, 67(1–2), 20–28. <https://doi.org/10.1016/j.gloplacha.2008.12.011>
- Wieder, W. R., Bonan, G. B., & Allison, S. D. (2013). Global soil carbon projections are improved by modeling microbial processes. *Nature Climate Change*, 3(10), 909–912. <https://doi.org/10.1038/nclimate1951>

- Willmott, C. J., Matsuura, K., & Legates, D. R. (2001). Terrestrial air temperature and precipitation: Monthly and annual time series (1950–1999). Center for climate research version, 1. Retrieved from [http://climate.geog.udel.edu/~climate/html\\_pages/download.html#ghcn\\_T\\_P\\_clim](http://climate.geog.udel.edu/~climate/html_pages/download.html#ghcn_T_P_clim)
- Yan, G., Qi, F., Wei, L., Aigang, L., Yu, W., Jing, Y., Aifang, C., et al. (2015). Changes of daily climate extremes in Loess Plateau during 1960–2013. *Quaternary International*, 371, 5–21. <https://doi.org/10.1016/j.quaint.2014.08.052>
- Yuan, X., Jian, J., & Jiang, G. (2016). Spatiotemporal Variation of Precipitation Regime in China from 1961 to 2014 from the Standardized Precipitation Index. *ISPRS International Journal of Geo-Information*, 5(11), 194.
- Zhao, M., & Running, S. W. (2010). Drought-Induced Reduction in Global Terrestrial Net Primary Production from 2000 Through 2009. *Science*, 329(6046), 940–943. <https://doi.org/10.1126/science.1199169>
- Zhao, Z., Peng, C., Yang, Q., Meng, F., Song, X., Epule, T. E., Li, P., et al. (2017). Model prediction of biome-specific global soil respiration from 1960 to 2012. *Earth's Future*, 5(7), 715–729. <https://doi.org/doi:10.1002/2016EF000480>